Experimental study and optimal control strategy of a transcritical CO_2 heat pump water heater

IOP Conf. Series: Materials Science and Engineering **604** (2019) 012059 doi:10.1088/1757-899X/604/1/012059

Experimental study and optimal control strategy of a transcritical CO_2 heat pump water heater

Zuliang Ye, Yikai Wang, Feng Cao

School of Energy and Power Engineering, Xi'an Jiaotong University, Xi'an 710049, China

E-mail: fcao@mail.xjtu.edu.cn

Abstract. In this study, a transcritical CO_2 heat pump water heater prototype was experimentally investigated in order to clarify the effects of the opening of electronic expansion valve (EEV), research the optimal discharge pressure and obtain an optimal control strategy for performance optimization. The tests were carried out by regulating the opening of EEV in multiple working conditions. The results showed that the decrease of opening led to reduction in evaporator inlet pressure and gas cooler outlet temperature, augment in discharge temperature, and decrease first then increase in discharge pressure. The optimal opening to reach maximum coefficient of performance (COP) always existed in all working conditions, however, there were two different situations where the corresponding optimal discharge pressure was near or away from the minimal value of the pressure curve. The reason for this phenomenon was the difference in water inlet temperature. Moreover, a correlation for the optimal discharge pressure was established with ambient temperature, water inlet and outlet temperature as independent variables. Furthermore, an optimal control strategy, in which the control of discharge pressure and superheat degree was considered, was proposed based on the correlation. Testing results proved that the optimization of performance could be achieved by using the strategy and the deviations between the COP under the control strategy and the optimal COP measured by experiments were within 5%.

1. Introduction

Compared with gas and electrical heating, heat pump is more energy-efficient for water heating. In terms of refrigerants, the HFCs need to be replaced due to their high global warming potential (GWP), and carbon dioxide (CO_2) has drawn more attention. CO_2 has extraordinary environmentally friendship (ODP=0, GWP=1), nontoxicity, incombustibility and excellent thermodynamic properties. Because of the high critical pressure and low critical temperature, CO_2 heat pump water heater generally operates in transcritical cycle where the high and low pressure side are in supercritical and subcritical regions, respectively. Moreover, the temperature glide during the supercritical exothermic process makes CO_2 fit perfectly for water heating and hot water could be produced more easily than traditional heat pumps.

As Zhang et al.[1] introduced, CO_2 heat pump water heater has been widely used in Japan. Khanam et al.[2] pointed out that the cost was still one of the most important problem that impeded adoption of the technology. Fernandez et al.[3] conducted full tank heating tests with CO_2 heat pump water heater in three scenarios of residential water heating, and the overall coefficient of performance (COP) was 30% higher for heating a full tank of cold water than reheating a warm tank water after standby losses. The

theoretically results of Nawaz et al.[4] illustrated that CO_2 heat pump had a comparable performance compared with R134a system especially when the separate hot water heat exchanger was adopted.

The discharge pressure significantly affects the performance of CO_2 system, and scholars have focused on the optimization of it. Kauf[5] stated that using graphical method to determine the optimal discharge pressure was time-consuming under multiple operating conditions, so Kauf determined the optimal discharge pressure as a function of gas cooler outlet temperature. After that, Liao et al.[6] and Sarkar et al.[7] obtained correlations for optimal discharge pressure in terms of gas cooler outlet and evaporation temperature. Qi et al.[8] presented an experimental investigation for a transcritical CO_2 heat pump water heater, and also established a correlation as function of gas cooler outlet temperature. Unlike previous authors, Wang et al.[9] got a correlation as function of ambient temperature and water outlet temperature instead of internal parameters. The correlation they got could be applied more robustly because the external parameters has less fluctuations than internal parameters like gas cooler outlet temperature.

Regarding to the optimal control of CO_2 heat pump, Kim et al.[10] developed a real-time optimal control method by comparing the predictive increment of specific cooling capacity with increment of specific work when discharge pressure was upraised, to determine whether COP would increase or not. The factors that caused inexact estimation, as they pointed out, were changes of gas cooler outlet temperature, evaporation pressure and compressor's suction enthalpy. Hu et al.[11] proposed a real-time strategy for minimizing the power consumption of a transcritical CO_2 heat pump that was capable to search and track optimal discharge pressure based on Extremum Seeking Control.

In this paper, the investigation focused more on the practical performance of the heat pump, and aimed to illustrate the effects of opening of EEV which is one of the most convenient control devices, and thereby propose an effective control strategy for performance optimization. For this purpose, a transcritical CO_2 heat pump water heater prototype was tested, and the effects of opening on different parameters were discussed. The optimal discharge pressure was researched and a correlation for it was established. An optimal control strategy considering control of discharge pressure and superheat degree was proposed based on the correlation. Compared to the well-known results in heat pump water heater, the contribution of this paper was distinct for the discussions about two situation of optimal discharge pressure and the control strategy we proposed.

2. Experimental system description

2.1. Testing prototype

The schematic diagram of the transcritical CO_2 heat pump water heater prototype is shown in Figure 1. The main components were compressor, gas cooler, electronic expansion valve, evaporator, filter and liquid-vapor separator. There were some temperature and pressure sensors on pipe lines, their measuring positions are also shown in Figure 1.

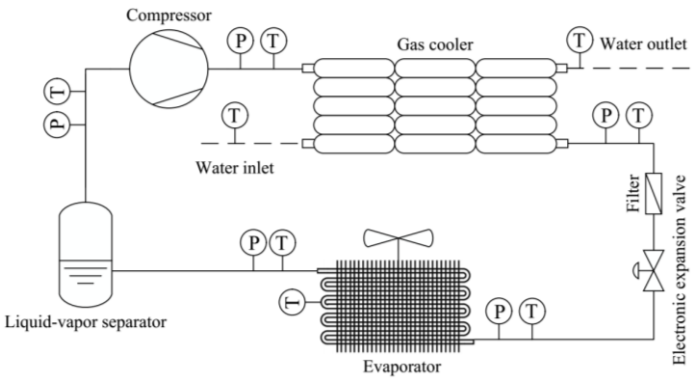

Figure 1. Schematic diagram of the transcritical CO_2 heat pump water heater prototype.

A semi-hermetic reciprocating compressor was used. The rated power, displacement and rotational speed of compressor were 20hp, 11.69 m^3/h and 1450 rpm, respectively. A spiral tube-in-tube gas cooler, consisting of three sets of counter flow heat exchangers, was used. The cross-sectional view of heat exchange tube is displayed in Figure 2. The heat exchange tube was made up of ϕ28×1.5mm outer stainless steel tube and spiral inner copper tube, in which water flowed in inner tube and CO_2 flowed in outer tube. The flow area ratio of inner tube to outer tube was 1.0 and the total heat transfer area was 4.26 m^2. The evaporator was composed of two same fin-tube heat exchangers. Each had four rows of copper tubes (ϕ7×0.7mm) and each row had 48 tubes. The thickness of wavy aluminum fins was 2.4 mm and spacing was 0.2 mm. The evaporator was equipped with two axial flow fans with rated power of 550W and rotational speed of 920 rpm. The EEV was controlled by a stepper motor, and the operation pulse range was 0 to 480 pulse. The inside volume of the liquid-vapor separator was 9.5 L.

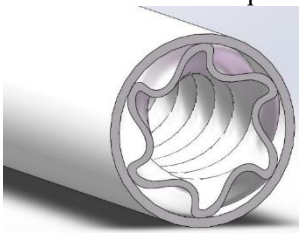

Figure 2. Cross-sectional view of the heat exchange tube used in gas cooler.

2.2. Testing chamber

The testing chamber included five parts: air conditioning system, water adjusting system, electric control system, data gathering system and environmental chamber. The air conditioning system controlled the ambient temperature and humidity in the chamber. The control range of ambient temperature was -25-55℃, and the accuracy was ±0.2℃. The water adjusting system controlled the water inlet temperature at set point with a range of 5-65℃ and the accuracy was ±0.2℃. A frequency-conversion water pump controlled the water flow rate and achieved control of water outlet temperature. The water outlet temperature could be up to 95℃. The parameters required to be measured contained temperature and pressure at different positions, water flow rate and electric power consumption. The details about control and measuring facilities are shown in Table 1.

Table 1. Details about control and measuring facilities.

Object	Facilities	Range	Accuracy
Ambient temperature	Air conditioning system	-25-55℃	±0.2℃
Water inlet temperature	Water adjusting system	5-65℃	±0.2℃
Water outlet temperature	Water adjusting system	Up to 95℃	±0.2℃
Temperature	T-type thermocouple and PT100 thermal resistance	-200-350℃	±0.5℃
Pressure	Pressure transmitter	0-15MPa	±2.5% of scale
Water flow rate	Electromagnetic flowmeter	0-6m^3/h	±0.5% of reading
Electric power consumption	Electric power analyzer	0-24kW	±(0.25% of scale+0.25% of reading)

3. Results and discussion

3.1. Effects of EEV's opening

During experiments, the prototype was tested by regulating the opening of EEV in multiple working conditions. The EEV's opening was presented as pulse of stepper motor, and the regulating pulse range was 0 to 480 pulse. The variations of different pressures and temperatures with variable opening of EEV are shown in Figure 3, where ambient temperature was 2℃, water outlet temperature was 70℃ and water inlet temperature was 10℃ or 40℃. $T_{w,in}$ means the water inlet temperature in ℃.

With decreased EEV's opening, the evaporator inlet pressure decreased. The decrease of opening narrowed the flow area of EEV and reduced the refrigerant flow rate into the evaporator. Meanwhile, the displacement of the compressor was mainly determined by its cylinder volume and hardly changed. Hence, to maintain the displacement, the evaporation pressure reduced and the suction density of compressor also decreased.

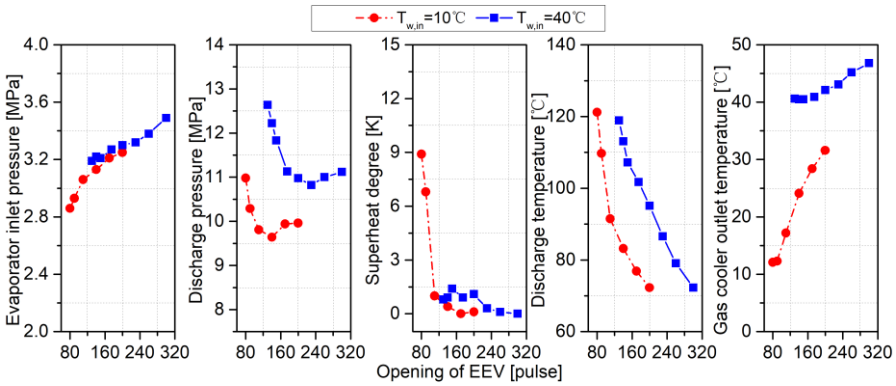

Figure 3. Variations of different pressures and temperatures with variable opening of EEV.

With decreased EEV's opening, the discharge pressure first decreased then increased. The reason for the trend of discharge pressure could be explained as below. When the opening was relatively large, the larger flow rate of refrigerant caused higher pressure drop in gas cooler and evaporator. Meanwhile, the spiral heat exchange tube used in gas cooler led to larger pressure drop due to its complex geometric shape. So the influence of pressure drop on high side pressure overwhelmed the influence of throttling when the opening was large. Conversely, when the opening was small, the throttling effect had a main influence on discharge pressure. The change of dominant factor for discharge pressure made the minimal value exist. Therefore, the discharge pressure was relatively high under large or small opening, and the minimum value existed under intermediate opening accordingly.

The superheat degree at evaporator outlet fluctuated near zero when opening of EEV was relatively large. With smaller opening, the superheat degree increased rapidly when $T_{w,in}$ was 10℃. But when $T_{w,in}$ was 40℃, the superheat degree stayed at a low level. As the opening reduced, the evaporation pressure and refrigerant mass flow rate decreased. Due to the same heat transfer area and increased temperature difference, the refrigerant in evaporator got more sufficient heat transfer and became superheated.

The discharge temperature increased with decrease of EEV's opening. When the opening decreased, although the discharge pressure didn't increased at first, the evaporation pressure decreased and the pressure ratio of compressor still increased. Also, the amount of refrigerant liquid at outlet of evaporator reduced because of reduced refrigerant mass flow rate. Thus, the discharge temperature kept increasing.

The gas cooler outlet temperature decreased with decrease of opening, and gradually approached $T_{w,in}$. The reduced refrigerant mass flow rate caused by decreasing the opening made the temperature glide in supercritical region more with same heat transfer area. And because of the heat transfer gradient, the gas cooler outlet temperature was impossible to be lower than $T_{w,in}$.

The heating capacity was the quantity of heat released by refrigerant to water in gas cooler, and could be written as the expression below:

$$Q_{gc} = c_{pw}\rho_w V\left(T_{w,out} - T_{w,in}\right) \tag{1}$$

Where Q_{gc} is the heating capacity in kW; c_{pw} is the isobaric specific heat of water in kJ·(kg·K)$^{-1}$; ρ_w is the density of water at the average temperature of inlet and outlet in kg·m^{-3}; V is the water volume flow rate in m^3/s; $T_{w,out}$ is the water outlet temperature in ℃.

The power consumption was the total electric power of prototype and was measured by an electric power analyzer. The COP was a parameter to describe the overall system performance, and was the ratio

of heating capacity to power consumption. The variations of heating capacity, power consumption and COP with variable opening of EEV are shown in Figure 4.

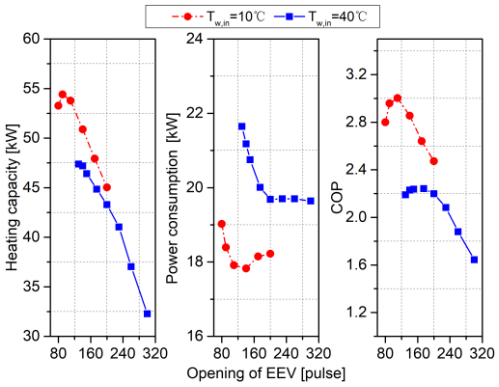

Figure 4. Variations of heating capacity, power consumption and COP with variable opening of EEV.

The existence of optimal COP resulted from variations of heating capacity and power consumption. With decrease of EEV's opening, the heating capacity first increased then decreased when $T_{w,in}$ was 10℃. When $T_{w,in}$ was 40℃, the heating capacity continued growing but the growing rate declined. When the opening was reduced, at first, the power consumption changed little when $T_{w,in}$ was 40℃, and even decreased when $T_{w,in}$ was 10℃. While it increased rapidly when the opening was smaller. Therefore, when opening was smaller than the optimal value, the decrease or slowing growth of heating capacity and augment in power consumption led to decrease in COP. The optimal opening was larger at higher water inlet temperature because when the prototype operated at higher water inlet temperature, the enthalpy difference between inlet and outlet of gas cooler was relatively small, and, consequently, the heating load reduced and the gas cooler could provide efficient heat exchanging for more fluid with the same heat transfer area. So the optimal opening of EEV should be larger for more refrigerant flow rate.

3.2. Two situations of optimal discharge pressure

In this section, the analysis of optimal discharge pressure was conducted. The variations of COP, heating capacity and power consumption with variable discharge pressure in different working conditions are shown in Figure 5. Similar to the curve of discharge pressure in Figure 3, the discharge pressure decreased first and then increased. With this trend of discharge pressure, the COP first increased and then decreased. The optimal discharge pressure at which the COP obtained maximum had two different situations: near or away from the minimal value of pressure. In two situations, the optimal discharge pressure both situated at the monotonic increasing segment.

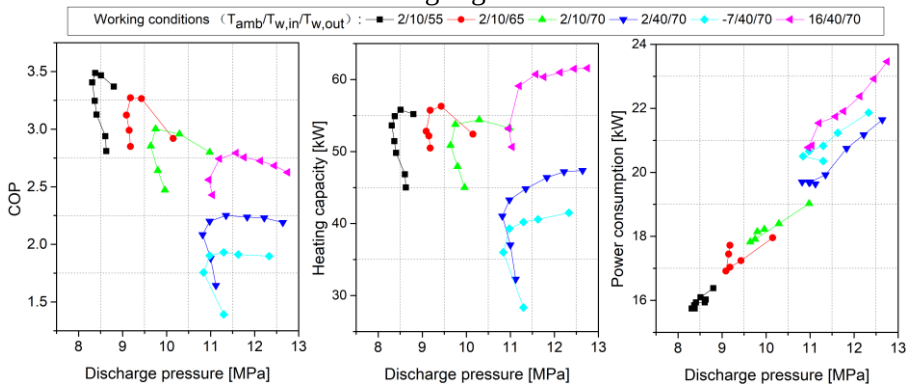

Figure 5. Variations of COP, heating capacity and power consumption with variable discharge pressure in different working conditions.

When $T_{w,in}$ was 10℃, the heating capacity decreased as soon as it passed the peak point. But when $T_{w,in}$ was 40℃, the heating capacity kept going up and the growth rate gradually slowed down. In terms of power consumption, with variable discharge pressure, it first decreased and then increased when $T_{w,in}$ was 10℃, and kept increasing when $T_{w,in}$ was 40℃.

When $T_{w,in}$ was 10℃, the optimal discharge pressure was close to the minimum value, because as the discharge pressure increased to more than the minimum value, the heating capacity decreased and the power consumption increased, making the COP drop rapidly. However, when $T_{w,in}$ was 40℃, the optimal discharge pressure was away from the minimum value, because as the discharge pressure rose, the heating capacity remained increasing, and COP could still increase. Until the growth of heating capacity was too slow and the power consumption rose rapidly, the COP started to decline but with a slower downward trend than that when $T_{w,in}$ was 10℃.

In P-h diagram, the heat pump cycles in two working conditions with increased discharge pressure are shown in Figure 6. The discharge pressures in two groups of cycles gradually increased from the lowest value. When the discharge pressure was risen, the enthalpy difference between inlet and outlet of gas cooler and compressor increased, and the mass flow rate of refrigerant decreased, simultaneously. The heating capacity of gas cooler and power consumption of compressor could be expressed based on enthalpy difference and mass flow rate of refrigerant as below:

$$Q_{gc} = m_r \left(h_{gc,in} - h_{gc,out} \right) \tag{2}$$

$$W_c = m_r \left(h_{dis} - h_{suc} \right) \tag{3}$$

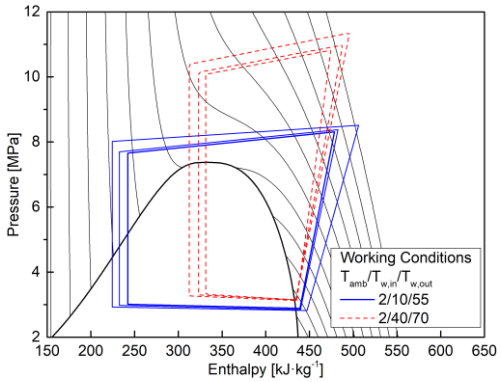

Figure 6. Cycles in two working conditions with increased discharge pressure in P-h diagram.

The augment in enthalpy difference tended to increase heating capacity and power consumption, and the reduction in refrigerant mass flow rate tended to decrease them. As for heating capacity, on one hand, when $T_{w,in}$ was 10℃, the enthalpy difference between inlet and outlet of gas cooler was large and thus increase of enthalpy difference only brought a small change. Therefore, the influence of augment in enthalpy difference was less than that of reduction in refrigerant mass flow rate, which led to decrease of heating capacity. On the contrary, when $T_{w,in}$ was high, because the enthalpy difference between inlet and outlet of gas cooler was smaller, the influence brought by increase of enthalpy difference was dominant, and it made the heating capacity risen. On the other hand, as the discharge pressure rose, the gas cooler outlet temperature would kept approaching $T_{w,in}$. The enthalpy of isothermal lines changed more at high temperature, which made the enthalpy difference increased more when gas cooler outlet temperature approached $T_{w,in}$ and increased heating capacity in some degree. Similar discussion could be made on the power consumption of compressor. The enthalpy difference between suction and discharge port of compressor was small, so the influence of increased enthalpy difference overwhelmed influence of decreased refrigerant mass flow rate, and power consumption increased accordingly.

Because of the physical properties of CO_2 in supercritical region, as shown in Figure 6, the isothermal lines was more sparse when the temperature is near critical point, and hence the enthalpy differences

between inlet and outlet of gas cooler changed dramatically when inlet temperature rose from below critical point to above. As a result, the boundary for the different trends of performance parameters was near the critical temperature. When inlet temperature was higher than critical temperature, the trends were more similar to those at 40℃. Otherwise, the trends were more similar to those at 10℃.

3.3. Optimal control strategy

In this paper, the prototype was controlled mainly by regulating the opening of EEV. And as the discussion above, the discharge pressure first decreased and then increased with decrease of opening. At the same time, the position of optimal discharge pressure in different working conditions had two situations: near or away from the lowest value.

In this case, if the prototype was controlled solely with discharge pressure as control objective, some problems would occur. Firstly, during controlling discharge pressure, the control modes of EEV under large opening and small opening were opposite. Under large opening, decreased opening caused decrease of discharge pressure. While under small opening, decreased opening caused increase of discharge pressure. Moreover, it was difficult to obtain the switching point for the two opposite control modes of EEV in different working conditions, which made the control more infeasible. Secondly, due to the variable trend of discharge pressure, when the optimal discharge pressure was near the lowest value, there might be two corresponding openings of EEV, which would hinder the control.

In order to solve these problems, an optimal control strategy, in which the control of both discharge pressure and superheat degree was considered, was proposed. Based on the experimental data in different working conditions, a correlation for optimal discharge pressure was established with ambient temperature T_{amb}, water inlet temperature $T_{w,in}$ and outlet temperature $T_{w,out}$ as independent variables, as below. The correlation was established by using the multiple linear regression analysis (R^2=0.979).

$$P_{opt} = 3.01557 + 0.00381T_{amb} + 0.05557T_{w,in} + 0.08934T_{w,out} \quad (4)$$

Where P_{opt} is the calculated optimal discharge pressure in MPa. The applicable range of the correlation was: ambient temperature -7-25℃; water inlet temperature 5-40℃; water outlet temperature 55-70℃. The coefficients of three external operating parameters are all positive, which showed the optimal discharge pressure would increase with increase of three parameters. In previous publications, the authors[5-8] mostly used gas cooler outlet temperature and evaporation temperature as independent variables. Wang et al.[9] adopted ambient temperature and water outlet temperature as independent variables. Compared with them, the correlation in this study took three external parameters as independent variables, which could eliminate the measuring errors caused by isolation of pipelines.

In terms of the superheat degree, the refrigerant at outlet of evaporator turned from two-phase to superheated gas as the EEV's opening decreased and discharge pressure passed through the lowest point. Hence, the existence of superheat degree could ensure the control mode of EEV was consistent. According to the contents above, an optimal control strategy was proposed and the control flow in single instance is shown in Figure 7. P_{dis} is the real-time measured discharge pressure in MPa; P_{opt} is the calculated optimal discharge pressure in MPa; T_{sh} is the superheat degree in K; ε is the allowable control error of discharge pressure in MPa. While using, the strategy was repeatedly continuous running in time.

T_{sh} is taken as control target at first. During the decrease of EEV's opening, if T_{sh} is larger than 5K, it could be guaranteed that the discharge pressure has passed the minimum value and the control mode of EEV is confirmed. Then P_{dis} is considered as control target and P_{opt} is calculated. If P_{dis} is larger than P_{opt}, turn up the opening of EEV; otherwise, if P_{dis} is smaller than P_{opt}, turn down the opening of EEV. P_{opt} should be calculated in real time according to the change of operating condition.

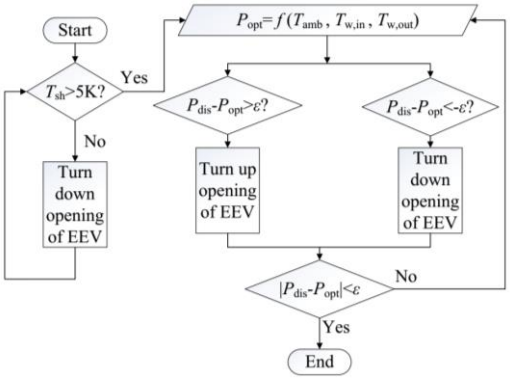

Figure 7. Control flow of the optimal control strategy in single instance.

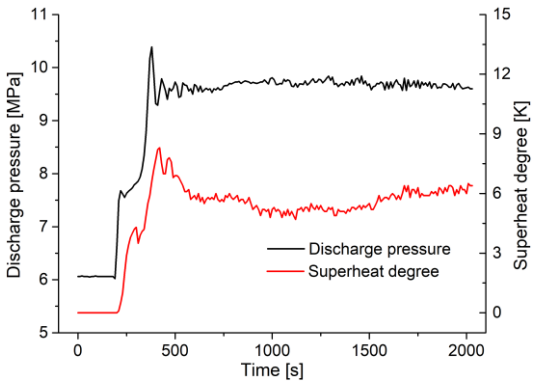

Figure 8. Typical control curves of discharge pressure and superheat degree.

The typical control curves of the strategy are displayed in Figure 8. It shows the variations of discharge pressure and superheat degree with time. The prototype started at 200s, the opening of EEV reduced to obtain enough superheat degree and the discharge pressure started rising. When the superheat degree reached 5K, the discharge pressure was set as control target and the opening of EEV was regulated based on the comparison between measured discharge pressure and calculated optimal discharge pressure. Over a period of time, the fluctuations of discharge pressure and superheat degree were caused by fluctuation of working condition.

The strategy was validated through tests. The results showed that the optimization of performance could be achieved when ε was 0.2 MPa. The deviations between the COP under the control strategy and the optimal COP measured by experiments were within 5%, and the control strategy could also adapt to operate in changing working condition. Compared to the method of previous publications, the advantages of the proposed strategy were the low requirement of measurement and control and the strong feasibility. The correlation for optimal discharge pressure was the core, and as the strategy in this paper was completely based on the experimental results, it was more in line with the need of practical application. However, due to the various pressure drop and heat transfer performance of components, the correlation should be adjusted when the strategy is applied in other systems.

4. Conclusion

In this paper, a transcritical CO_2 heat pump water heater prototype was experimentally studied. Through the tests, the effects of EEV's opening on system performance were researched, the optimal discharge pressure was investigated and an optimal control strategy was proposed.

With decrease of EEV's opening, the discharge pressure first decreased then increased, the evaporator inlet pressure decreased, the discharge temperature increased, the gas cooler outlet temperature decreased and gradually approached water inlet temperature. The superheat degree fluctuated near zero when opening of EEV was relatively large. When the opening was smaller, the superheat degree increased rapidly when water inlet temperature was 10℃. But when water inlet temperature was 40℃, the superheat degree stayed at a low level.

The optimal opening of EEV always existed in all working conditions but the corresponding optimal discharge pressure had two different situations: near or away from the minimal value of discharge pressure. When water inlet temperature was 40℃, the optimal discharge pressure was away from the minimum value; otherwise, when water inlet temperature was 10℃, the optimal discharge pressure was close to the minimum value.

Based on experimental data, a correlation for optimal discharge pressure was established with ambient temperature, water inlet temperature and water outlet temperature as independent variables. In addition, an optimal control strategy, in which the control of both discharge pressure and superheat degree was considered, was proposed. Testing results showed that the optimization of performance

could be achieved and the deviations between the COP under the control strategy and the optimal COP measured by experiments were within 5%.

References

[1] Zhang J F, Qin Y, Wang C C. 2015. Review on CO_2 heat pump water heater for residential use in Japan. *Renewable and Sustainable Energy Reviews*, **50**:1383-91.
[2] Khanam M, Daim T U. 2017. A regional technology roadmap to enable the adoption of CO_2 heat pump water heater: A case from the Pacific Northwest, USA. *Energy Strategy Reviews*, **18**:157-74.
[3] Fernandez N, Hwang Y, Radermacher R. 2010. Comparison of CO_2 heat pump water heater performance with baseline cycle and two high COP cycles. *International Journal of Refrigeration*, **33**(3):635-44.
[4] Nawaz K, Shen B, Elatar A, et al. 2018. Performance optimization of CO_2 heat pump water heater. *International Journal of Refrigeration*, **85**: 213-28.
[5] Kauf F. 1999. Determination of the optimum high pressure for transcritical CO_2-refrigeration cycles. *International Journal of Thermal Sciences*, **38**(4):325-30.
[6] Liao S, Zhao T, Jakobsen A. 2000. A correlation of optimal heat rejection pressures in transcritical carbon dioxide cycles. *Applied Thermal Engineering*, **20**(9):831-41.
[7] Sarkar J, Bhattacharyya S, Gopal M R. 2004. Simulation of a transcritical CO_2 heat pump cycle for simultaneous cooling and heating applications. *International Journal of Refrigeration*, **29**(5):735-43.
[8] Qi P C, He Y L, Wang X L, et al. 2013. Experimental investigation of the optimal heat rejection pressure for a transcritical CO_2 heat pump water heater. *Applied Thermal Engineering*, **56**(1-2):120-5.
[9] Wang S, Tuo H, Cao F, et al. 2013. Experimental investigation on air-source transcritical CO_2 heat pump water heater system at a fixed water inlet temperature. *International Journal of Refrigeration*, **36**(3):701-16.
[10] Kim M S, Shin C S, Kim M S. 2014. A study on the real time optimal control method for heat rejection pressure of a CO_2 refrigeration system with an internal heat exchanger. *International Journal of Refrigeration*, **48**:87-99.
[11] Hu B, Li Y, Wang R Z, et al. 2018. Real-time minimization of power consumption for air-source transcritical CO_2 heat pump water heater system. *International Journal of Refrigeration*, **85**: 395-408.